Journal of Luminescence 191 (2017) 61–67

Contents lists available at ScienceDirect

Journal of Luminescence

journal homepage: www.elsevier.com/locate/jlumin

Intraband luminescence excited in new ways: Low-power x-ray and electron beams

Sergey I. Omelkov [a,*], Vitali Nagirnyi [a], Eduard Feldbach [a], Rosana Martinez Turtos [b], Etiennette Auffray [c], Marco Kirm [a], Paul Lecoq [c]

[a] Institute of Physics, University of Tartu, W. Ostwaldi Str. 1, Tartu 50411, Estonia
[b] Università degli Studi di Milano Bicocca, Piazza della Scienza 3, 20126, Milano, Italy
[c] CERN, Geneva 23, CH-1211, Switzerland

ARTICLE INFO

Article history:
Received 17 October 2016
Received in revised form
18 January 2017
Accepted 1 February 2017
Available online 3 February 2017

ABSTRACT

Hot intraband luminescence (IBL) was observed under excitation by high-power (120 keV, 10 A/cm^2) pulsed electron beam, low-energy (10 keV) and low-current (2 μA) continuous electron beam as well as pulsed x-rays. Thus, the fundamental possibility of IBL excitation by x-rays was confirmed, and for most studied materials the absence of the dependence of IBL spectral shape on excitation energy was revealed. For the first time, the intraband luminescence was monitored under low-power excitation, which confirmed the absence of a power threshold of its mechanism and completely ruled out the role of excitation density effects in IBL formation. The data obtained allow the prediction that the IBL can be excited by single photons of 511-keV energy, which is required for enhancing scintillation time resolution in TOF-PET.

1. Introduction

Intraband luminescence (IBL) is a prompt emission originating from the radiative intraband transitions of electrons (e-IBL) and holes (h-IBL) during thermalisation following their creation by ionizing radiation [1]. Despite its relatively low yield the IBL can hopefully enhance scintillation time resolution by providing an almost instant time marker for the scintillation event, for instance, in time-of-flight positron emission tomography (TOF-PET) [2]. TOF-PET requires the detection of single photons of 511-keV energy with exceptionally high time resolution (10–100 ps). IBL is capable of providing such time resolution, as its decay time is determined by the interplay between the probabilities of radiative transitions and phonon relaxation (thermalisation) of charge carriers, which takes place within the picosecond time scale. However to date, there have been no reports on the reliable observation of IBL under 511-keV photon excitation. The radioluminescence decay curves of some scintillators have been studied with sufficient time resolution to detect prompt emissions, however, the IBL could not be distinguished from the Čerenkov light produced by secondary electrons [3]. Therefore, a Čerenkov-free experiment is required to figure out whether IBL can be excited by x-ray or γ-radiation.

So far, the primary excitation sources for studying IBL have been the pulsed electron guns utilizing the field electron emission effect [4]. Scarce complementary data were obtained with a pulsed laser excitation [5]. Pulsed electron guns provide excitation pulses with relatively high peak power. For example, the peak electron current density was up to 2000 A/cm^2 in [4], 100 A/cm^2 in [6], 10–100 A/cm^2 in [7], while our laboratory setup provides about 50 A/cm^2 [8]. Electron pulses of high peak power can be expected to create electronic excitations at high densities, however, the currently accepted model of IBL [1] does not consider it as an energy density effect; neither power threshold for its excitation is expected. Up to now, no observations of IBL have been reported under low-peak-power excitations.

The observations of IBL under x-ray excitation have been scarce and the results controversial. In [9,10], a prompt wide-band cathodoluminescence (CL) of Al_2O_3 has been reported to depend on the energy of exciting electrons. The spectra presented in a wavelength scale were flat in the range 200–1400 nm under excitation by the 300 keV electrons. When the excitation energy was lowered, the CL spectrum narrowed so that at 7 keV the flat spectrum transformed into a narrow band peaking at 380 nm (3.2 eV). The emission spectra of Al_2O_3 under soft x-ray (1–3 keV) and femtosecond VUV laser (16.6–18.2 eV) excitations were also represented by a similar narrow band [11,12]. However, the electron beam currents as well as x-ray and laser power in these works were up to 2000 kA/cm^2 and 10^{12}–10^{13} W/cm^2, respectively, which is significantly higher than in all the works cited above. Other

* Corresponding author.
E-mail address: omelkovs@gmail.com (S.I. Omelkov).

http://dx.doi.org/10.1016/j.jlumin.2017.02.001
0022-2313/

authors [6] have reported different results on the spectrum of the prompt ($\tau < 20$ ps) component of the CL of Al_2O_3, which demonstrated two peaks at 2.05 and 2.5 eV. No observations of the spectra of IBL have been performed with the x-ray excitation energies above 10 keV and densities below 10^8 W/cm^2.

The present research is aimed at the observation of intraband luminescence under low-current electron beam and pulsed x-ray excitation in order to confirm the possibility of IBL excitation with x-rays in principle and to demonstrate the absence of low-pulse-power threshold for IBL emission.

2. Experimental

2.1. Apparatus and setup

The luminescence spectra under high-power pulsed electron beam and x-ray excitation were recorded using a pulsed electron beam setup described in detail in [8]. It was build around a RADAN-303A electron gun, which works by applying pulsed high voltage (100–200 keV) across the cathode-anode gap. During a sub-nanosecond (~300 ps) voltage pulse, the beam is formed due to the field electron emission effect. In this work, we used electrons with maximum energy of 120 keV either directly as an excitation beam or with a converter foil to obtain x-ray pulses (Fig. 1, a). In both cases, the excitation was strongly non-monochromatic. The spectrum of a generated electron beam was estimated using the time profiles of the cathode-anode gap voltage and electron beam current, carefully synchronized taking into account all delays in the measurement circuits. The voltage profile gives the energy of electrons in a particular time moment, while the beam current is proportional to the number of electrons emitted at that moment. The histogram of voltage values distribution weighted by current values is an approximation of the electron spectrum reaching the anode foil. Such approach was used for similar electron guns in [4] and [13]. The spectrum of electron beam in the sample chamber after passing through the anode foil (25 μm Al) was calculated using the Geant4 library with Livermore physics model [14] (Fig. 1, b). In x-ray luminescence experiments, x-rays were obtained by bombarding a 25 μm Cu, Mo, Ag or Sn converter foil with the same electron beam. The filter foil (250 μm Be) was placed directly after the converter foil to absorb any remaining electrons from the beam in order to obtain a pure x-ray excitation. Both the Geant4 simulations and the measurements of the charge accumulated by a Faraday cup placed instead of a sample have shown that the amount of electrons passing the filter is insignificant. Geant4 was also used to model the spectrum of x-rays hitting the sample (Fig. 1, b) for various materials of converter foil. The spectrum is dominated by the characteristic emission line, which constitutes about 40–50% of the total intensity, while the rest is a higher energy braking radiation with a broad spectrum. Unlike the characteristic emission, the braking radiation hardly depends on converter foil material and comprises the photons with energy above 30 keV, which constitute about 30% of the total number of all emitted photons. The peak electron current at the anode foil was 60 A/cm^2, and pulse width ~250 ps. The quantum efficiency of electron to x-ray conversion was estimated by Geant4 as 2×10^{-3}. In cathodoluminescence studies, the variation of electron current (and thus excitation density) was realized by moving a sample mounted in a cryostat further away from the anode foil. In the case of both x-ray and electron beam excitation, the front sample face was irradiated, while the luminescence photons were registered from the opposite one (Fig. 1, a). Several cathodoluminescence measurements were performed in other geometries in order to compare the results of different experiments (see Section 3.2). A reflective collimator was used to collect light and focus it onto the input slit of an Andor Shamrock SR303i spectrograph. This collimator provides a significant improvement in light collection efficiency compared to the quartz lens used in our previous work [8]. It also substantially reduced the radiation load on the cryostat optical window. For light detection, Hamamatsu R3809U-50 MCP-PMT or H10330A-75 NIR detectors were used in pulse current mode with a LeCroy SDA 760Zi-A oscilloscope. An iStar DH 720_18 mm gated iCCD camera was also available for the study of time-resolved spectra. The further details on the detector operation and data treatment have been given in [8].

The CL spectra under continuous and pulsed low-current excitation were obtained using a continuous monochromatic electron gun (Kimball Physics EGG-3101, $E_e = 10$ keV, $I_e = 2.0$ μA) with a focused beam (~1 mm^2 spot on the sample). An ARC Spectra Pro 2300i monochromator with a Hamamatsu H8259SEL photon counting head (dark count rate <3 cps) were used as a registration system in the UV-visible range. For the study of emission decay kinetics the gun is equipped with a beam blanker, which forms 10 ns wide square pulses with the repetition rate of 5 kHz. The peak electron current in the pulse does not exceed 2.0 μA. A Becker& Hickl MSA-300 Multiscaler card was used for decay curve recording. All decay curves were recorded with an equal exposure of 10^6 pulses. A 3 nm platinum coating was applied to the sample surface, preventing the accumulation of electric charge during the measurements. The continuous glow of the heated Y_2O_3 cathode of the electron gun was recorded separately and subtracted from the measured emission spectra. Its impact is low and noticeable only below 2.5 eV (Fig. 5, curve 5). In this setup, the electron beam was exciting the same sample face luminescence photons were registered from (see Fig. 7, geometry 1).

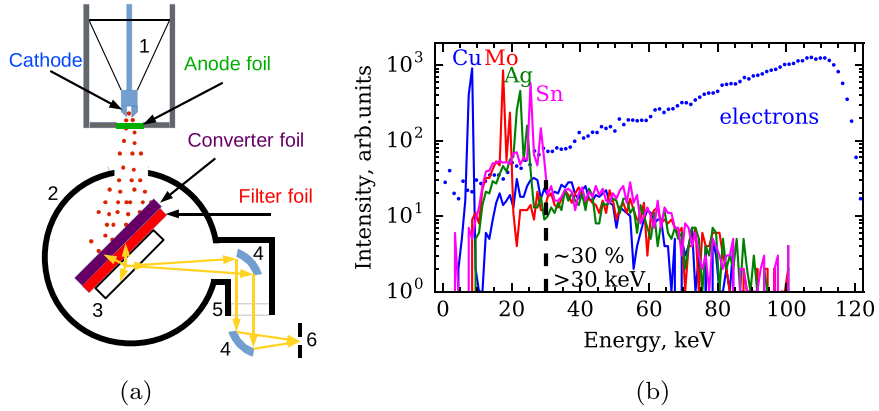

Fig. 1. The experiment layout for x-ray luminescence (a), and the Geant4-simulated spectra of various excitation beams (b). The anode foil is 25 μm Al, the converter foil is 25 μm Cu, Mo, Ag or Sn, and the filter foil is 250 μm Be. For cathodoluminescence experiments the converter and filter foils are removed. 1-electron gun, 2-vacuum cryostat, 3-sample, 4-off-axis parabolic mirrors (Al+MgF_2), 5-fused silica window, 6-monochromator input slit.

All luminescence spectra were corrected for the spectral sensitivity of the detection systems. The correction method has been described in detail [8]. The y-scale of all graphs is labeled dN/dE, which means the number of photons dN per second per unit spectral interval dE in the energy scale.

We also made an attempt to detect IBL using a picosecond x-ray luminescence setup in CERN [15]. A 40 kV x-ray tube with a laser-excited photocathode and tungsten anode provided pulses of 134 ps FWHM at 4 MHz repetition rate. Average tube current was 2 μA, and the strongest characteristic x-ray emission lines were at ~10 keV. For luminescence detection, a Hamamatsu C10910 streak camera was utilized. The streak images containing information on both scintillation spectrum and time profile were recorded for CsI, $PbWO_4$, $Lu_3Al_5O_{12}$ and $CaWO_4$. No prompt emission could be revealed within the setup sensitivity. For $CaWO_4$, the prompt emission detection threshold was estimated relative to the intensity of the main excitonic band based on 3σ of the setup noise level. At the main emission peak wavelength 420 nm the threshold was estimated to be 6×10^{-4} of the main excitonic emission intensity (see Fig. 4, a).

2.2. The excitation density

When studying the changes in the properties of IBL caused by the transition from a high-density electron beam to lower density x-ray excitation, it is important to ensure that the density of the electron beam is below the threshold of causing the response saturation of a scintillation material, as it was observed for IBL in alkali halides in [4]. We have recorded the dependence of the luminescence intensity of BGO on charge density transmitted to the sample by one electron pulse (Fig. 2). It was discovered that at the maximum peak beam current (60 A/cm^2) of our setup the nonlinear response of BGO is evident. This current density is equivalent to the charge of 15 nC/cm^2 per pulse, which is rather small compared to the IBL nonlinearity threshold discovered in [4] (50–100 nC/cm^2). However, the excitation pulse in the latter case was 10 times longer, resulting in much lower excitation densities at the same charge values. The linearity range for both IBL and the main scintillation band in our case extended at least up to 2.5 nC/cm^2 per pulse (10 A/cm^2), so this value was selected for all the pulsed cathodoluminescence experiments in this study.

The excitation density delivered to the sample was estimated for all the three above-described excitation types. For the pulsed electron beam, 10 A/cm^2 peak current density equivalent to 1.5×10^{10} electrons/cm^2 per pulse was used. The penetration depth of 100 keV electrons in most heavy scintillators is on the order of 20 μm, so the volume energy density induced by one pulse is about 10^{15} keV/cm^3. For the continuous electron beam the current of 2 μA applied over a 1 mm^2 spot gives 2×10^{-4} A/cm^2 or 10^{15} electrons/cm^2/s. The penetration depth in this case is on the order of 500 nm, yielding 10^{20} keV/cm^3 per second or 10^{11} keV/cm^3 per 250 ps time interval. For x-ray generation, 60 A/cm^2 peak current density was used, and converted into 1.8×10^9 x-ray photons/cm^2 per pulse. The attenuation length of 17-keV x-rays (Mo converter foil) is about 20 μm in heavy scintillators, while more energetic photons will only penetrate further, leading to the decrease of an average density. Therefore, the upper limit is 10^{12} keV/cm^3 per pulse. Thus, the excitation density of both x-rays and continuous electron beam were 10^3–10^4 times lower than that of the pulsed electron beam used in our experiment. The excitation density of a picosecond x-ray luminescence setup in CERN is even smaller than that. The average x-ray tube current of 2 μA translates to 3x10^6 electrons/cm^2 per pulse. Assuming the conversion efficiency of 10^{-3} similar to x-ray conversion in the foil as described above, an upper limit of 10^8 keV/cm^3 is estimated.

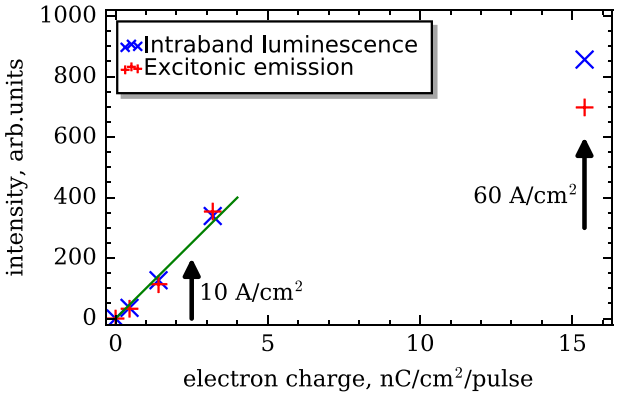

Fig. 2. The dependence of luminescence intensity of excitonic emission (pluses) and IBL (crosses) of BGO sample on the charge density transmitted to the sample by the electron beam. Arrows indicate maximum peak electron current 60 A/cm^2 of the gun and selected working current 10 A/cm^2 for cathodoluminescence experiments. The solid line shows the linearity range. T=298 K.

2.3. Sample selection

To compare the light output and spectrum shape of IBL at different excitations and to estimate its yield, we needed some other emission in the same sample as a standard with known yield, as direct absolute light output measurements are not possible with our instrumentation. In the best case, this could be a well-studied scintillation emission having proportional response with respect to excitation particle energy. For this purpose we have selected a sample of $Bi_4Ge_3O_{12}$ (BGO) which features a wide scintillation band with rather slow non-exponential decay and the yield of about 8500 ph/MeV [16]. It could be easily separated from IBL by time resolution. The main emission of BGO has been shown to be of excitonic nature and its decay kinetics has been carefully studied in [17]. In addition, BGO features a fair proportionality of scintillation yield in the 10–100 keV energy range, which does not fall below 70% of the standard yield value measured at 662 keV [18]. Another material featuring similar excitonic emission is $CaWO_4$, possessing slower decay and rather similar scintillation yield of 16200 ph/MeV [19].

However, with a continuous beam excitation the only way to distinguish IBL from other emissions is spectral resolution. The yield of IBL is roughly 10^{-4} as compared to the yield of the main emissions in bright scintillating materials [1]. As typical stray light suppression in Czerny-Turner monochromators is also similar to this value, the spectral resolution can be used only if the main emissions are absent or very weak. We decided in favor of $BaWO_4$ as a test material for this experiment, as it does not possess an intrinsic excitonic emission, while defect emissions are strongly quenched at room temperature [20]. An actual level of a stray light was estimated by measuring the detector count rate at 6.5 eV, where an air-filled monochromator does not transmit any monochromatic light. This value was subtracted from the measured spectra. Another good example of a material missing intrinsic excitonic emissions is cubic PbF_2 sometimes utilized as Čerenkov detector [21]. A single crystal of PbF_2 used in this study did not possess any detectable extrinsic emissions either.

3. Results and discussion

3.1. Pulsed electron beam and x-ray excitation

Fig. 3 shows the luminescence spectra of BGO and $BaWO_4$ under electron beam and x-ray excitation, normalized to the same intensity of the main scintillation band. In all cases, the spectra

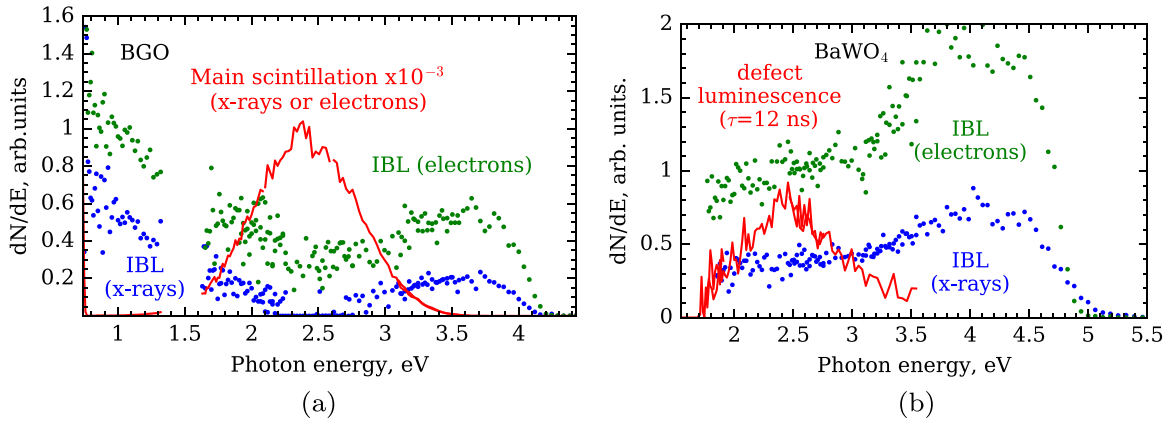

Fig. 3. The luminescence spectra of BGO (a) and $BaWO_4$ (b) under pulsed electron beam and x-ray (Mo converter foil) excitation, normalized to the same intensity of the main excitonic band (BGO) or defect emission ($BaWO_4$). T=298 K.

and relative yield of IBL were the same irrespective of the foil (Cu, Mo, Ag and Sn) used for the pulsed x-rays generation. However, the relative intensity of IBL as compared to that of other emissions at x-ray excitation was about twice as low as at electron beam excitation. On the contrary, the shape of the IBL spectrum did not depend significantly on the excitation type. Only in the case of $CaWO_4$ (Fig. 4a) there are slight differences in the 1.5–3 eV energy range between IBL spectra obtained with electron beam and x-ray excitation. Fig. 4b shows also the spectra of PbF_2 recorded using an iCCD. As this material does not possess any other emission, the iCCD-spectra recorded in a fast time window 0–32 ns after the excitation pulse are a direct measurement of the IBL spectra themselves without any mathematical processing. In the 2–4 eV range, the spectral shapes are exactly the same, while there are minor differences in the 4–5 eV region. Those differences might be caused by relatively short-living absorption due to radiation damage induced by an electron beam, which delivers a higher dose as compared to x-rays. The radiation effects induced in PbF_2 by low-energy gamma and neutron irradiation have been found to influence the near-edge transmission and to vanish in a few days or after UV irradiation [21,22].

It is not yet known which features of electronic band structure influence the shape of the IBL spectrum. PbF_2 demonstrates almost flat spectrum, implying that the transitions of various energies within the conduction or valence band are of equal probability. The study of the photoelectron spectra of PbF_2 has shown that its valence band is barely structured [23]. Besides, as the width of the PbF_2 valence band E_v is comparable to E_g [24], one can not distinguish between electron and hole transitions in the spectrum like it has been done for wide-gap oxides in [25]. The IBL spectrum of $BaWO_4$, on the other hand, has a very prominent hump at 3.5–4.5 eV. It has been reported that the peculiarities of the IBL spectrum can sometimes reflect the valence band structure in the case it demonstrates clearly separated sub-bands [26]. The DFT calculations of the band structure of $BaWO_4$ [27] have shown that its valence band may be split in two parts separated by approximately 2.5 eV. The upper sub-band consists mainly of the 2*p* states of oxygen, while the lower one has a significant contribution of the 4*d* states of tungsten. One can suggest that the radiative transitions between the sub-bands are more allowed than the transitions within the upper sub-band alone, which leads to an increased intensity of the IBL spectrum in high-energy region. The calculated energy gap between the centers of sub-bands is about 2.5 eV, which seems to be too low value to describe the observed hump at 3.5–4.5 eV in the IBL spectrum. However, the DFT calculations used in [27] do not give accurate positions for the *d*-states lying deeper in the valence band. On the example of $CdWO_4$ R. Laasner has shown that more accurate GW-approximation gives the positions of all *d*-states at significantly lower energies (up to 0.5 eV lower for 4*d* W and 1 eV lower for 4*d* Cd), while the XPS measurements demonstrate even deeper position of 4*d* Cd states [28]. Therefore, it is highly probable that the actual location of 4*d* states of tungsten in $BaWO_4$ is 1–1.5 eV lower than anticipated by [27], and transitions between the sub-bands of the valence band

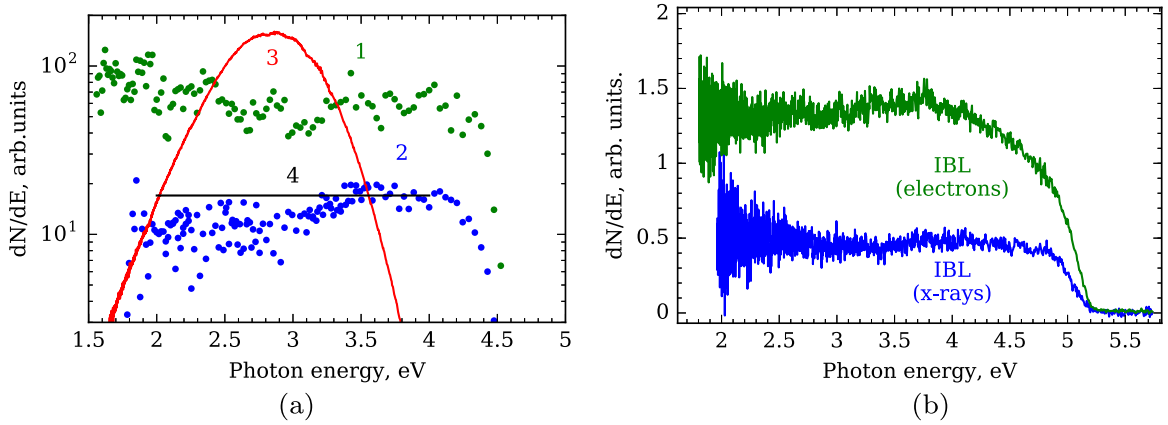

Fig. 4. (a) The IBL spectra of $CaWO_4$ under electron beam (1) and x-rays (Sn converter foil, 2), normalized to the same intensity of the main excitonic band (3), which is shown scaled down by 10^3. The 3σ detection threshold for IBL of the picosecond x-ray experiment in CERN calculated relative to the main excitonic band is shown by horizontal line (4). (b) The IBL spectra of PbF_2 under electron beam and x-ray (Mo converter foil) excitation, recorded by iCCD in 0–32 ns time window relative to the excitation pulse. Normalized arbitrarily, T=298 K.

yield an increase of IBL intensity in the UV spectral region. In the case of $CaWO_4$ the gap between 2*p* states of oxygen and 4*d* states of tungsten is less prominent [27], and its IBL spectrum is flatter similar to that of PbF_2(especially under electron beam excitation).

3.2. $BaWO_4$ under low-current electron beam excitation

Fig. 5 shows the luminescence spectra of $BaWO_4$ under continuous excitation by an electron beam (10 keV, 2 μA) in a logarithmic scale. The decay curves obtained with a beam blanker are shown in Fig. 6. The band at 2.5 eV is a defect emission, the intensity and decay time of which are strongly temperature dependent [20]. However, the spectra have a shoulder at 3.8–4.7 eV whose intensity does not depend on temperature. Above the fundamental absorption edge of the material, which shifts towards higher energies on cooling, the intensity of this shoulder drops by almost an order of magnitude. The spectrum recorded by iCCD under excitation by a high-power pulsed electron beam in the same geometry (curve 4) displays a cutoff at the same energy (about 4.75 eV) as the spectrum obtained with continuous beam at the same temperature (300 K, curve 2). The decay curves of this emission recorded at E_{em}=4.3 eV, being the same at T=300 and 400 K, show only 3 data points which are greatly above the background (Fig. 6, right panel). As each point represents a 5 ns-wide channel, and the excitation pulse is 10 ns-wide, we can obtain such decay curve only if its shape matches an excitation pulse profile. At T=78 K the defect band is much stronger and its contribution is significant even at 4.3 eV, which is visible on Fig. 6 (right panel, topmost curve) as a slower decay component. However, its impact at 4.75 eV is substantially diminished and the decay curve matches the excitation pulse again. A remarkably weak non-stray light possessing a very fast time profile is emitted also at the energies above the fundamental absorption edge (e. g., at 5.6 eV). Such high-energy emission can be observed only under the specific conditions, when the emission from the excited area exclusively is detected, while the emission exiting the crystal after multiple reflections is masked. Using the 100 keV electron excitation (Fig. 7), we were able to show that it is indeed a surface-specific effect. A similar emission with energies slightly above the fundamental absorption edge have been detected also in $CaWO_4$ [7] and $CdWO_4$ [29] under excitation by the 300 keV electrons. According to the modeling with the WinXray program [30], 10 keV electron beam is completely absorbed at the depth of about 600 nm in $BaWO_4$, but near a quarter of electrons does not penetrate deeper than 200 nm. This is less than the wavelength of the emitted light, leaving a possibility for it to escape the crystal even though the absorption coefficient is very high. The 100 keV beam penetrates up to 40 μm deep with less significant energy deposit at the near-surface layer. For that reason, the intensity of the above-described high-energy emission is much lower in the latter case (Fig. 5, curve 4) even if a proper experiment geometry is assured.

The relative intensity of IBL as compared to the defect emission is by at least an order of magnitude lower in case of the 10 keV excitation than that in the case of the 100 keV excitation. As at the 100 keV excitation the decay constant of the 2.8 eV emission is

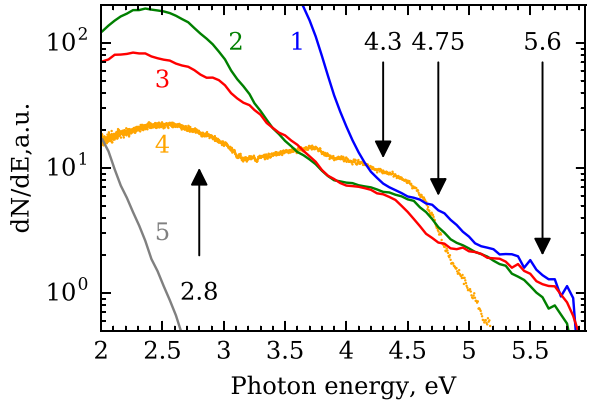

Fig. 5. The luminescence spectra of $BaWO_4$ under continuous excitation by electron beam (10 keV, 2 μA) at T=79 K (1), 300 K (2) and 400 K (3). For comparison, a spectrum under high-power pulsed electron beam (100 keV, 40 A/cm^2) recorded at T=300 K in the 0-32 ns time window is also presented (4). Curve (5) shows the glow spectrum of heated yttria cathode of electron gun. Arrows indicate energies at which the decay curves are recorded.

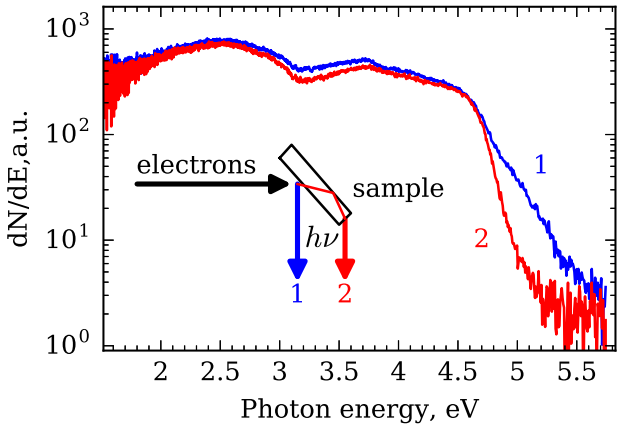

Fig. 7. The CL spectra of $BaWO_4$, recorded in a fast (0-32 ns) time window for two different geometries (1,2) as illustrated. High-power pulsed electron beam (100 keV, 40 A/cm^2) is used as excitation, T=298 K.

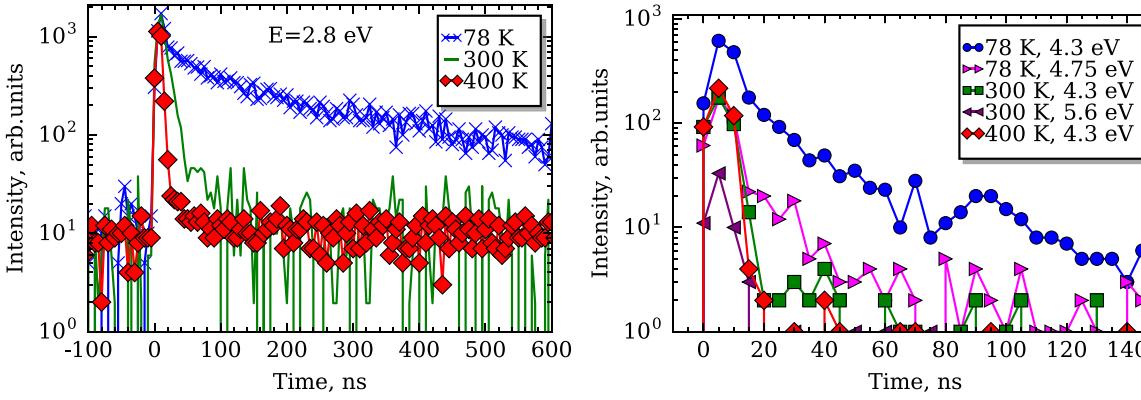

Fig. 6. The decay curves of $BaWO_4$ emission under pulsed (10 ns, 5 kHz) excitation by electron beam (10 keV, 2 μA). Sample temperature and emission energy are indicated in figures.

τ=13 ns at T=300 K, a 0–32 ns time window selects almost all of the 2.8 eV emission, as there were no slower decay components observed in the decay kinetics. The background in the decay curves shown in Fig. 6(left panel) is determined solely by the continuous glow of the heated cathode of the electron gun, so no significant longer components are observed with the 10 keV electrons either. Therefore, the difference in yields is not explained by the different timing settings of the experiments.

In conclusion of this section, the spectra observed under the excitation by the 10 keV electrons demonstrate the emission with all the characteristics specific to IBL: the decay times which are much shorter than the time resolution of the setup, a flat spectrum with the cutoff at the fundamental absorption edge, insignificant temperature dependence of intensity. We can thus affirm that for the first time an IBL was observed under low-peak-power excitation, confirming within the studied power range the absence of a power threshold for its mechanism.

3.3. Discussion

The experimental results shown above indicate clearly the fundamental possibility of the excitation of IBL in different materials by a low-peak-power electron beam and x-rays. However, the yield of IBL as compared to that of excitonic and defect emissions is significantly different with all the three excitation types. An obvious trend of the relative yield is to decrease when the excitation energy is decreased. This trend explains also why no differences in the IBL yield were observed at x-ray excitations generated from the 120 keV electron beam with different x-ray converter foils. As the biggest contribution in the yield is made by the higher-energy breaking radiation, which does not depend on foil material, it is expected that lower-energy characteristic x-ray emission lying in the range of 8–22 keV does not excite a significant portion in the total yield of IBL despite its dominating role in the x-ray spectrum. The situation is similar to the case of electron excitation, at which the light yield with the 10 keV electron beam is below 10% of the one with 100 keV. In the case of even lower-energy x-ray beam (<40 keV), utilized at the setup in CERN, the IBL intensity was also low so it could not be detected above the 3σ of a noise level.

As the excitation methods utilized in this study were different, one can not completely exclude other effects possibly making contribution to the observed yield differences. According to the WinXray program [30], the excited layer thickness of a $BaWO_4$ sample is only 600 nm in the case of 10 keV electrons. As the surface layer contains more defects than bulk, its contribution to the spectra at the excitation by 10 keV electrons may be higher than in the case of 100 keV electrons, which penetrate much deeper in the material. Therefore, at the present study stage we cannot draw conclusions about possible IBL yield nonlinearity on excitation energy. This problem, being a very interesting topic from the fundamental point of view, has not yet been touched in scientific literature at all. The available models of a non-proportional scintillator response have been focused on the nonlinear quenching processes due to the interaction of both hot and thermalized quasiparticles [31]. As the mechanism of IBL is related only to hot charge carriers, the studies of the IBL non-proportionality are potentially able to reveal the peculiarities of the quenching processes at the stages preceding thermalization. The experimental data can be compared to the results of a systematic theoretical study of the thermalization time and diffusion range of hot electrons in selected scintillators, which has been recently published [32].

The 511-keV single photon excitation utilized in TOF-PET application differs from the high-power pulsed electron beam excitation usually used for the studies of IBL in two essential ways: the particle type and the excitation density. The data obtained in this paper have shown that neither of these differences are critical for the IBL formation, therefore it is highly probable that prompt IBL is emitted also under 511-keV single photon excitation along with Čerenkov radiation produced by secondary electrons.

4. Conclusions

For the first time, the intraband luminescence was observed in different materials under low-peak-power excitation, confirming the absence of a low power threshold of its mechanism and completely ruling out excitation density effects as the reason for IBL formation. We have confirmed that the IBL can be excited by x-rays and its spectra are qualitatively similar to those obtained with high-power electron beam excitation. $BaWO_4$ have revealed similar spectra of the prompt emission under excitation by 10 and 100 keV electrons. The data show possible yield nonlinearity of IBL on excitation energy, which deserves a separate study. One of important outcomes of the present study is a conclusion that it seems reasonable to expect that the IBL can also be excited by single photons of 511-keV energy, and therefore it is suitable for enhancing scintillation time resolution in TOF-PET. The important question, whether the interaction with 511-keV photon will produce enough prompt photons for the application, will be addressed in the future research.

Acknowledgements

This work has been inspired by Crystal Clear Collaboration and supported by Estonian Research Council (projects PUT1081, IUT2-26). Picosecond x-ray experiment in CERN was supported by an STSM Grant from the COST Action TD1401 “FAST” and ERC Advanced Grant no. 338953 (TICAL).

References

[1] D. Vaisburd, S. Kharitonova, Two types of fundamental luminescence of ionization-passive electrons and holes in optical dielectrics – intraband-electron and interband-hole luminescence (theoretical calculation and comparison with experiment), Russ. Phys. J. 40 (11) (1997) 1037–1060, http://dx.doi.org/10.1007/BF02508940.

[2] P. Lecoq, M. Korzhik, A. Vasiliev, Can transient phenomena help improving time resolution in scintillators? Nucl. Sci. IEEE Trans. 61 (1) (2014) 229–234, http://dx.doi.org/10.1109/TNS.2013.2282232.

[3] S. Gundacker, E. Auffray, K. Pauwels, P. Lecoq, Measurement of intrinsic rise times for various L(Y)SO and LuAG scintillators with a general study of prompt photons to achieve 10 ps in TOF-PET, Phys. Med. Biol. 61 (7) (2016) 2802.

[4] D.I. Vaisburd, B.N. Semin, E.G. Tavanov, S.B. Matlis, I.N. Balychev, G.I. Gering, High-energy solid-state electronics, Novosibirsk, Izdatel'stvo Nauka, 1982, in Russian.

[5] R. Deich, M. Karklina, L. Nagli, Intraband luminescence of CsI crystal, Solid State Commun. 71 (10) (1989) 859–862, http://dx.doi.org/10.1016/0038-1098(89)90212-3.

[6] R. Deich, M. Abdrakhmanov, Picosecond radiation induced processes in wide-gap crystals, Nucl. Inst. Methods Phys. Res. B 65 (1992) 525–529, http://dx.doi.org/10.1016/0168-583x(92)95099-d.

[7] V. Nagirnyi, E. Feldbach, L. Jönsson, M. Kirm, A. Lushchik, C. Lushchik, L. L. Nagornaya, V.D. Ryzhikov, F. Savikhin, G. Svensson, I.A. Tupitsina, Excitonic and recombination processes in $CaWO_4$ and $CdWO_4$ scintillators under synchrotron irradiation, Radiat. Meas. 29 (3–4) (1998) 247–250, http://dx.doi.org/10.1016/S1350-4487(98)00017-1.

[8] S.I. Omelkov, V. Nagirnyi, A.N. Vasil'ev, M. Kirm, New features of hot intraband luminescence for fast timing, J. Lumin. 176 (2016) 309–317, http://dx.doi.org/10.1016/j.jlumin.2016.03.039.

[9] V. Baryshnikov, T. Kolesnikova, Femtosecond mechanisms of electronic excitations in crystalline materials, Phys. Solid State 47 (10) (2005) 1847–1851, http://dx.doi.org/10.1134/1.2087734.

[10] V.I. Baryshnikov, L.I. Shchepina, T. Kolesnikova, E.F. Martynovich, Wide-band fast-response luminescence of oxide single-crystals excited by heavy-current electron beams, Fiz. Tverd. Tela 32 (6) (1990) 1888–1890.

[11] V. Baryshnikov, T. Kolesnikova, S. Dorokhov, Interaction of high-power x rays

with sapphire crystals and quartz based materials, Phys. Solid State 39 (2) (1997) 250–253, http://dx.doi.org/10.1134/1.1129793.
[12] V. Baryshnikov, T. Kolesnikova, Mechanisms of femtosecond energy transfer upon strong excitation in crystals, Opt. Spectrosc. 95 (4) (2003) 594–598, http://dx.doi.org/10.1134/1.1621444.
[13] M.J. Rhee, G.T. Zorn, R.C. Placious, J.H. Sparrow, Studies of electron beams from a Febetron 705, IEEE Trans. Nucl. Sci. 18 (3) (1971) 468–472, http://dx.doi.org/10.1109/TNS.1971.4326090.
[14] J. Allison, K. Amako, J. Apostolakis, H. Araujo, P.A. Dubois, M. Asai, G. Barrand, R. Capra, S. Chauvie, R. Chytracek, G.A.P. Cirrone, G. Cooperman, G. Cosmo, G. Cuttone, G.G. Daquino, M. Donszelmann, M. Dressel, G. Folger, F. Foppiano, J. Generowicz, V. Grichine, S. Guatelli, P. Gumplinger, A. Heikkinen, I. Hrivnacova, A. Howard, S. Incerti, V. Ivanchenko, T. Johnson, F. Jones, T. Koi, R. Kokoulin, M. Kossov, H. Kurashige, V. Lara, S. Larsson, F. Lei, O. Link, F. Longo, M. Maire, A. Mantero, B. Mascialino, I. McLaren, P.M. Lorenzo, K. Minamimoto, K. Murakami, P. Nieminen, L. Pandola, S. Parlati, L. Peralta, J. Perl, A. Pfeiffer, M. G. Pia, A. Ribon, P. Rodrigues, G. Russo, S. Sadilov, G. Santin, T. Sasaki, D. Smith, N. Starkov, S. Tanaka, E. Tcherniaev, B. Tome, A. Trindade, P. Truscott, L. Urban, M. Verderi, A. Walkden, J.P. Wellisch, D.C. Williams, D. Wright, H. Yoshida, Geant4 developments and applications, IEEE Trans. Nucl. Sci. 53 (1) (2006) 270–278, http://dx.doi.org/10.1109/TNS.2006.869826.
[15] R. Turtos, S. Gundacker, A. Polovitsyn, S. Christodoulou, M. Salomoni, E. Auffray, I. Moreels, P. Lecoq, J. Grim, Ultrafast emission from colloidal nanocrystals under pulsed x-ray excitation, J. Instrum. 11 (2016) P10015, http://dx.doi.org/10.1088/1748-0221/11/10/P10015.
[16] M. Moszynski, M. Kapusta, M. Mayhugh, D. Wolski, S.O. Flyckt, Absolute light output of scintillators, IEEE Trans. Nucl. Sci. 44 (3) (1997) 1052–1061, http://dx.doi.org/10.1109/23.603803.
[17] M. Itoh, T. Katagiri, Intrinsic luminescence from self-trapped excitons in $Bi_4Ge_3O_{12}$ and $Bi_{12}GeO_{20}$: decay kinetics and multiplication of electronic excitations, J. Phys. Soc. Jpn. 79 (7) (2010) 074717.
[18] I.V. Khodyuk, P. Dorenbos, Trends and patterns of scintillator nonproportionality, IEEE Trans. Nucl. Sci. 59 (6) (2012) 3320–3331, http://dx.doi.org/10.1109/TNS.2012.2221094.
[19] M. Moszynski, M. Balcerzyk, W. Czarnacki, A. Nassalski, T. Szczesniak, H. Kraus, V. Mikhailik, I. Solskii, Characterization of $CaWO_4$ scintillator at room and liquid nitrogen temperatures, Nucl. Instruments Methods Phys. Res. Sect. A Accel. Spectrometers Detect. Assoc. Equip. 553 (3) (2005) 578–591, http://dx.doi.org/10.1016/j.nima.2005.07.052.
[20] R. Laasner, V. Nagirnyi, S. Vielhauer, M. Kirm, D. Spassky, V. Sirutkaitis, R. Grigonis, A.N. Vasil'ev, Cation influence on exciton localization in homologue scheelites, J. Phys. Condens. Matter 27 (38) (2015) 385501, http://dx.doi.org/10.1088/0953-8984/27/38/385501.
[21] D. Anderson, M. Kobayashi, C. Woody, Y. Yoshimura, Lead fluoride: an ultracompact Cherenkov radiator for em calorimetry, Nucl. Instruments Methods Phys. Res. Sect. A Accel. Spectrometers Detect. Assoc. Equip. 290 (2) (1990) 385–389, http://dx.doi.org/10.1016/0168-9002(90)90553-I.
[22] P. Kozma, R. Bajgar, P.K. Jr., 2002. Radiation resistivity of PbF_2 crystals, Nuclear Instruments and Methods in Physics Research Section A: Accelerators, Spectrometers, Detectors and Associated Equipment 484 (13), 149–152. http://dx.doi.org/10.1016/S0168-9002(01)02011-3.
[23] M. Itoh, Valence-band structures of lead halides by ultraviolet photoelectron spectroscopy, J. Fac. Eng. Shinshu Univ. 80 (1999) 19–28 (URL ⟨http://ci.nii.ac.jp/naid/110000237339/en/⟩).
[24] H. Jiang, R. Orlando, M.A. Blanco, R. Pandey, First-principles study of the electronic structure of PbF_2 in the cubic, orthorhombic, and hexagonal phases, J. Phys. Condens. Matter 16 (18) (2004) 3081, http://dx.doi.org/10.1088/0953-8984/16/18/009.
[25] A. Lushchik, F. Savikhin, I. Tokbergenov, Fast intrinsic emissions of wide-gap oxides under electron irradiation, Radiat. Eff. Defects Solids 158 (1–6) (2003) 305–308 (9th Europhysical Conference on Defects in Insulating Materials, WROCLAW, POLAND, JUL 01-05, 2002.).
[26] F. Savikhin, M. Kerikmäe, E. Feldbach, A. Lushchik, D. Onishchik, D. Rakhimov, I. Tokbergenov, Fast intrinsic emission with the participation of oxyanion and cation excitations in metal sulphates, Physica Status Solidi (C.) 2 (1) (2005) 252–255, http://dx.doi.org/10.1002/pssc.200460158.
[27] R. Lacomba-Perales, D. Errandonea, A. Segura, J. Ruiz-Fuertes, P. Rodríguez-Hernández, S. Radescu, J. López-Solano, A. Mujica, A. Muñoz, A combined high-pressure experimental and theoretical study of the electronic band-structure of scheelite-type AWO_4 (A=Ca, Sr, Ba, Pb) compounds, J. Appl. Phys. 110 (4) (2011) 043703, http://dx.doi.org/10.1063/1.3622322.
[28] R. Laasner, G_0W_0 band structure of $CdWO_4$, J. Phys. Condens. Matter 26 (12) (2014) 125503.
[29] V. Nagirnyi, E. Feldbach, L. Jönsson, M. Kirm, A. Kotlov, A. Lushchik, L. Nagornaya, F. Savikhin, G. Svensson, Study of oriented $CdWO_4$ scintillating crystals using synchrotron radiation, Radiat. Meas. 33 (5) (2001) 601–604, http://dx.doi.org/10.1016/S1350-4487(01)00067-1.
[30] R. Gauvin, E. Lifshin, H. Demers, P. Horny, H. Campbell, Win x-ray: a new monte carlo program that computes x-ray spectra obtained with a scanning electron microscope, Microsc. Microanal. 12 (2006) 49–64, http://dx.doi.org/10.1017/S1431927606060089.
[31] X. Lu, Q. Li, G.A. Bizarri, K. Yang, M.R. Mayhugh, P.R. Menge, R.T. Williams, Coupled rate and transport equations modeling proportionality of light yield in high-energy electron tracks: CsI at 295 K and 100 K; CsI:Tl at 295 K, Phys. Rev. B 92 (2015) 115207, http://dx.doi.org/10.1103/PhysRevB.92.115207.
[32] H. Huang, Q. Li, X. Lu, Y. Qian, Y. Wu, R.T. Williams, Role of hot electron transport in scintillators: a theoretical study, Physica status solidi (RRL) Rapid Res. Lett. 10 (10) (2016) 762–768, http://dx.doi.org/10.1002/pssr.201600276.